A. Puškár
Critical strain amplitudes, elasticity modulus defect and fatigue life

# Critical Strain Amplitudes, Elasticity Modulus Defect and Fatigue Life

A. PUŠKÁR*)

Czechoslovakia

Measuring of internal friction in the region, where it is progressively dependednt on strain amplitude gives oportunity to evaluate also the elasticity modulus $E$ and its changes described by the elasticity modulus defect $\Delta E/E$. New approximation gives possibility to evaluate the stress amplitude $\sigma_a$ as well as plastic strain amplitude $\varepsilon_{ap}$. When $\sigma_a$ and $\varepsilon_{ap}$ are calculated at different values of total strain amplitude $\varepsilon_{at}$, which is higher than second critical strain amplitude, i.e. when cumulation of fatique demage is in progress, it is possible to construct the curve $\sigma_a$ vs $\varepsilon_{ap}$ and describe it by equation $\sigma_a = \varkappa \cdot \varepsilon_{ap}^n$, where $n$ is coefficient of cyclic deformation hardening.

## Introduction

From the aspects of assessing the cyclic microplasticity of metals, many useful data are provided by the curve of internal damping dependence $Q^{-1}$ as well as the
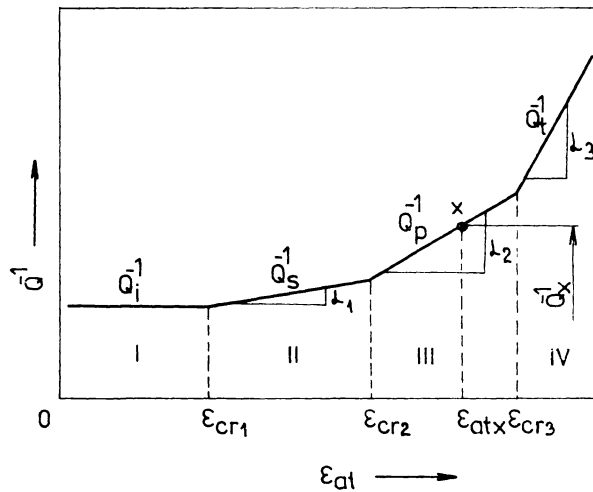


Fig. 1. Scheme dependence of internal damping on total strain amplitude.

*) Department of Materials Science, University of Transport and Communication, 010 26 Žilina, Czechoslovakia,

curve of elasticity modulus defect $\Delta E/E$ on the total strain amplitude $\varepsilon_{at}$, as schematically shown in Fig. 1 and Fig. 2.
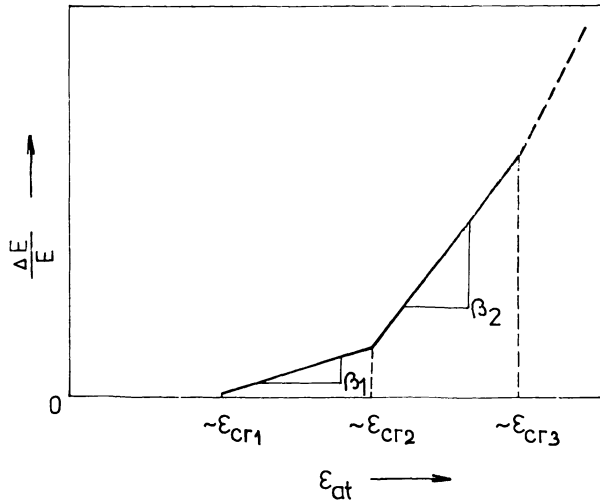


*Fig. 2.* Scheme dependence of elasticity modulus defect on total strain amplitude.

### Internal damping and elasticity modulus defect

Conventionally, we have divided the dependence $Q^{-1}$ vs. $\varepsilon_{at}$ into four parts. When strain amplitudes act with a magnitude up to $\varepsilon_{cr1}$ (part I) internal damping $Q_i^{-1}$, independent on the value of $\varepsilon_{at}$ is identified. This value of $Q_i^{-1}$ is also labelled as a phon of internal damping and is interpreted by utilizing one or several of the mechanisms already presented [1]. The applied stress amplitude being too small to make the dislocation segments swing. In this region elasticity modulus defect does not take place, i.e. $\Delta E/E = 0$ (Fig. 2). Value of $\varepsilon_{cr1}$ is the first critical strain amplitude. When strain amplitudes act with a magnitude higher then $\varepsilon_{cr1}$ (part II), the internal damping $Q_s^{-1}$ is found to depend slightly on $\varepsilon_{at}$. The rise of internal damping in this portion of the dependence $Q^{-1}$ vs. $\varepsilon_{at}$ is characterised by factor $\alpha_1$ and is interpreted as the inelastic interaction of dislocation segments with energetic barriers. Dislocation segments are vibrating in a quasiviscous environment produced by point defects and phonons.

The bond energy between the dislocation and the alloying element atoms $(r)$ is embodied in the equation [2] in the form $\varepsilon_{cr1} = rc/b^3 E$, where $c$ is the concentration of alloying element atoms around dislocation and $b$ is the Burgers vector.

In this portion of the dependence $\Delta E/E$ vs. $\varepsilon_{at}$ it is possible to register also some values of elasticity modulus defect, which slightly depends on the $\varepsilon_{at}$ by the proportional factor of $\beta_1$ (Fig. 2). The elasticity modulus defect at some value of $\varepsilon_{cr1} \leqq$

126

$\leqq \varepsilon_{at} \leqq \varepsilon_{cr2}$ has been characterised by the equation [3] $\Delta E/E = 6\,\Omega\,NL^2/\pi^2$, where $\Omega$ is orientation factor, $N$ is density of dislocation. Quantity of $L$ is the effective dislocation length determined by equation $1/L = 1/L_N + 1/L_C$, $L_N$ is the entire length of the locked dislocation segment and $L_C$ is the distance between the locking points formed by the solute atoms. Increase of $\Delta E/E$ with increase of $\varepsilon_{at}$ illustrates the redistribution of locking points and thus also the rise of effective dislocation length.

When strain amplitudes exceeding $\varepsilon_{cr2}$ (part III) are acting, the internal damping $Q^{-1}$ depends markedly on the strain amplitude. It is also labelled "plastic" internal damping. Value of $\varepsilon_{cr2}$ is a second critical strain amplitude. The dislocation sources start generating dislocations which overcome the barriers. Process of increase of dislocation density depends on the value of $\varepsilon_{at}$. In this portion, proportional factor between $Q_p^{-1}$ and $\varepsilon_{at}$ is labelled $\alpha_2$ which characterized, first of all, the dynamics of dislocation density changes. Here changes in dislocation density and structural sensitive physical and mechanical properties of materials started. It exhibits a saturating character, i.e. following a definite number of loading cycles, $Q_p^{-1}$ stabilizes at a certain value and it is assumed that density and distribution of dislocation no longer change significantly at some value of $\varepsilon_{at}$. At value of $\varepsilon_{cr2} \leqq \varepsilon_{at} \leqq \varepsilon_{cr3}$ it is registered a strong rise of $\Delta E/E$ at increase of $\varepsilon_{at}$, i.e. high value of proportional factor of $\beta_2$.

The second critical strain amplitude corresponds to the stress causing the generation dislocation, i.e. $\sigma_{cr2} = Eb/L_N$ [4] where $b$ is the Burgers vector, then $\varepsilon_{cr2} = b/L_N$.

In the region of "plastic" internal damping following equation is valid $(\Delta E/E)^2/$ $/Q_p^{-1} = kN$, where $k$ is a correlation factor and $N$ is the immediate density of dislocation in the material [5].

The application of strain amplitudes exceedings $\varepsilon_{cr3}$ (part IV) causes a process of fatigue damage cummulation, internal damping $Q_t^{-1}$ thus being a function of loading time, or at some loading frequency also the number of loading cycles. Value of $\varepsilon_{cr3}$ is a third critical strain amplitude. It may be assumed that in this portion there is proportional factor $\alpha_3$, which is also dependent on the time of loading. Experimental data and interpretation for part IV have so far hardly been published, if only because there are other procedures that supplemented the method of internal damping measurement.

Values of $\varepsilon_{cr1}$ and $\varepsilon_{cr2}$ and propably also $\varepsilon_{cr3}$ are some boundaries, where some mechanisms of energy dissipation in material change. Because action of different mechanisms is connected with orientation factor of grains in polycrystals for start and propagation of cyclic microplasticity strain these values are more or not conventionally extrapoled values.

The behaviour of the $Q^{-1}$ vs. $\varepsilon_{at}$ as well as $\Delta E/E$ vs. $\varepsilon_{at}$ dependences is a function of many substructural and structural factors and of the material type, composition, and material proceedings, whereby all three critical strain amplitudes may (but need not) be recorded, depending on the sensitivity of the $Q^{-1}$, or $\Delta E/E$ measurement and on the overlapping of various partial mechanisms of mechanical energy dissipation.

For high-frequency loading, around 20 kHz, it is impossible to evaluate the plastic strain amplitude $\varepsilon_{ap}$ directly from experiments for the time being. This is reason for Puškár's approximation [6], which exploited resonance principle of measuring of internal damping (Fig. 3).
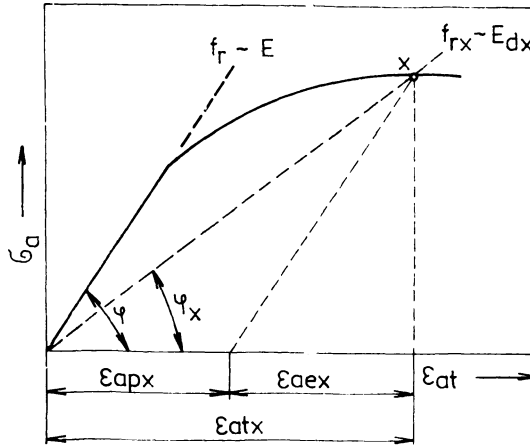


*Fig. 3.* Scheme of stress-strain relation.

In the elastic region $\sigma_a = E\varepsilon_{ac}$. Resonance system with the specimen has the basic resonance frequency $f_r$ which corresponding to the value $E$ ($\sim \operatorname{tg}\varphi$). In the elastic-plastic region i.e. upper value of $\varepsilon_{cr2}$ (e.g. for point $x$) we have $\sigma_{ax} = E_x(\varepsilon_{aex} + \varepsilon_{ap}x) = E_x\varepsilon_{atx}$ the resonance frequency of the system $f_{rx}$, corresponding to the value $E_x(\sim \operatorname{tg}\varphi_x)$. Then $E_x = E - \Delta E_x$, where $\Delta E_x$ is the change of elasticity modulus connected with the microplastic deformation of the specimen. Then

(1)
$$\sigma_a = E\varepsilon_{at}\left(1 - \frac{\Delta E}{E}\right).$$

and

(2)
$$\varepsilon_{ap} = \varepsilon_{at}\left(\frac{\Delta E}{E}\right).$$

### Fatigue characteristics

Cyclic plastic reaction of material on the external loading may be expressed by equation for cyclic stress-strain curve in the form $\sigma_a = \varkappa\varepsilon_{ap}^{n'}$, where $\varkappa$ is a structurally and experimentally dependent constant (e.g. on loading frequency) and $n'$ is the coefficient of cyclic strain-hardening.

128

It can be seen that eqs. (1,2) and eq. for cyclic stress-strain curve make a bridge between elasticity modulus defect and cyclic microplasticity reaction of material.

The „plastic" internal damping $Q_p^{-1}$ ($= Q_x^{-1} - Q_{cr2}^{-1}$, where $Q_x^{-1}$ and $Q_{cr2}^{-1}$ are values of internal damping at some value of $\varepsilon_{atx}$ and $\varepsilon_{cr2}$ — see Fig. 1) may be embodied as the ratio of the energy dissipation in one cycle of loading $\Delta W = F\sigma_a\varepsilon_{ap}$, where $F$ is the characteristic of the hysteresis loop shape, and the total applied energy $W = 1/2 \, E\varepsilon_{at}^2$. Then

$$Q_p^{-1} = \frac{\Delta W}{2\pi W} = \frac{F\sigma_a\varepsilon_{ap}}{E\varepsilon_{at}^2} \, . \tag{3}$$

The amplitude of plastic strain also be expressed by the eq.

$$\varepsilon_{ap} = \left( \frac{\pi Q_p^{-1} E\varepsilon_{at}^2}{F\varkappa} \right)^{\frac{1}{n'+1}} \, . \tag{4}$$

Here is also the way how to evaluate the factor of the hysteresis loop shape using eq.

$$F = \frac{\pi Q_p^{-1}}{\dfrac{\Delta E}{E} \left( 1 - \dfrac{\Delta E}{E} \right)} \, . \tag{5}$$

It may be mentioned that eqs. from (1) to (4) are valid in the region of $Q^{-1}$ vs. $\varepsilon_{at}$ at values of $\varepsilon_{cr2} \leqq \varepsilon_{at} \leqq \varepsilon_{cr3}$. For some materials which have strong binding between intersticial solute atoms and dislocations some cyclic limits [7], schematically presented in Fig. 4b, were shown. Cyclic loading with stress amplitude below limit of cyclic elasticity stress amplitude $\sigma_{ace}$ is characterised by reversibility and hence only by an elastic reaction of the material on cyclic loading. No changes in the material
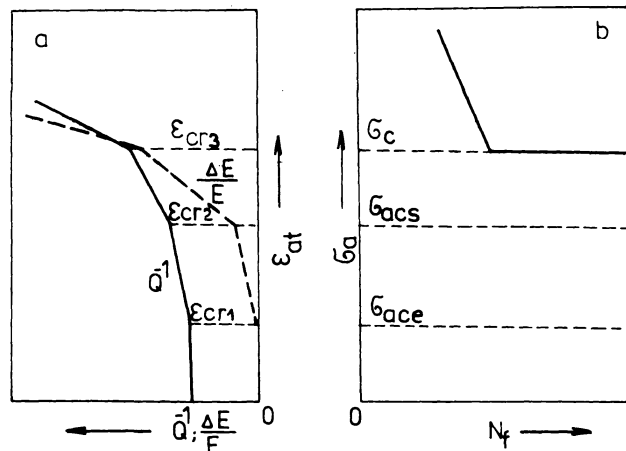


*Fig. 4.* Scheme dependence of $Q^{-1}$ and $\Delta E/E$ on $\varepsilon_{at}$ (a) and stress amplitude on number of cycles to fracture (b).

occur beneath this stress level. When quantity of $\sigma_a$ is upper limit of cyclic sensitivity stress amplitude $\sigma_{acs}$ and under the fatigue limit of $\sigma_c$ incurs changes in the dislocation structure with saturation behaviour.

## New hypothesis

Phenomenological similarities of dislocation behaviour at the interpretation of dependence $Q^{-1}$ vs. $\varepsilon_{at}$ or $\Delta E/E$ vs. $\varepsilon_{at}$ and that of $\sigma_a$ vs. $N_f$ (where $N_f$ si number of cycles to fracture) make it possible to formulate a new hypothesis, by following equations

$$\sigma_{ace} = E_d \varepsilon_{cr1} , \tag{6}$$

$$\sigma_{acs} = \varkappa^+ \left( \varepsilon_{cr2} \frac{\Delta E}{E} \right)^{n^+} \tag{7}$$

and

$$\sigma_c = \varkappa' \left( \varepsilon_{cr3} \frac{\Delta E}{E} \right)^{n'} , \tag{8}$$

where $E_d$ is a dynamic elasticity modulus. It can be assumed that for region where $\varepsilon_{cr1} \leqq \varepsilon_{at} \leqq \varepsilon_{cr2}$ values of $\varkappa^+$, $n^+$ are characteristics factors of stress-strain curve and these are not the same for the region $\varepsilon_{cr2} \leqq \varepsilon_{at} \leqq \varepsilon_{rc3}$, where these are labelled as $\varkappa'$, $n'$. Of quite dubious character is the equation (8), because value of $\varepsilon_{cr3}$ have not been proved for the time being.

## References

[1] PUŠKÁR, A., GOLOVIN, S. A.: Vnútorné tlmenie materiálov. ALFA Bratislava, 1990.
[2] WEINIG, S., MACHLIN, E.: J. Appl. Phys., 27, 1956, 734.
[3] NATSUNE, H., SHIMIZU, G., SAKOMOTO, M.: J. Phys. Soc. Japan, 21, 1966, 560.
[4] GRANATO, A. LÜCKE, K., J. Appl. Phys., 27, 1958, 583, 789.
[5] MÜLLNER, H., BAJONS, P., KOUSEK, H., WEISS, B.: In Fifth Int. Conf. Internal Friction and Ultrasonics Attenuation in Crystalline Solids, Vol. 2, Springer-Verlag New York, 1976, 376..
[6] PUŠKÁR, A.: Ultrasonics (London), May 1982, 118.
[7] IVANOVA, V. S., Izv. AN SSSR, Ser. Metall. Topl., 1960, 1, 93.

# Microplasticity of High $T_c$ Superconductors in the Temperature Range 77 — 300 K

L. S. FOMENKO,*) H.-J. KAUFMANN,**) S. V. LUBENETS,*) V. D. NATSIK,*) T. S. ORLOVA,***) N. N. PESCHANSKAYA,***) V. V. SHPEIZMANN,***) B. I. SMIRNOV***)

USSR, Germany

Characteristics of the microplasticity are investigated in HTSC's by two methods — microindentation and microcreep. The microhardness $H_v$ increases by approximately 50—80 % when decreasing temperature from 300 to 77 K. The temperature dependence $H_v(T)$ is the weaker, the higher indentation load. This may be due to an intergrain slip contribution to local strain. The dependence $H_v(T)$ does not display any peculiarity at the transition of ceramic to a superconducting state within the limits of experimental accuracy. There maxima between 77 and 300 K and corresponding to changes in the mobility of structure defects are the important peculiarities of the temperature spectra of inelastic deformation rate measured at compression of ceramic samples by laser interferometer. The maximum at $T \simeq 90$ K is probably associated with the superconducting transition.

## Introduction

The study of the mechanical properties of HTSCs is accomplished via two different techniques: (a) microindentation and (b) microcreep. Microindentation is utilized to measure the microhardness and the microbrittleness of single crystals and ceramics of some rare-earth cuprates RBCO (R: Y, Gd, Ho, Dy, Er, Yb) and Bi-containing HTSCs, as well as to study anisotropy of indenter induced strain and crack formation in single crystals. Microcreep is employed to investigate the peculiarities of inelastic deformation of YBCO ceramics in superconducting and normal states.

## Experimental

*Single crystals.* Composition, structure, parameter difference, $\Delta = b - a$, and critical temperature, $T_c$, of RBCO crystals are given in the Table. Samples 1 were

---

*) Institute for Low Temperature Physics and Engineering, Academy of Sciences of the Ukrain. SSR, Kharkov, USSR.

**) Institute of Semiconductor Physics, Low Temperature Lab., Academy of Sciences of GDR, Berlin, Germany.

***) A. F. Ioffe, Physico-Technical Institute, Academy of Sciences of USSR, Leningrad, USSR.

$0.5 \times 0.5 \times 0.3$ mm$^3$, the rest of the samples were thin plates $1 \times 1 \times (0.1-0.2)$ mm$^3$ of a smaller dimension along the axis c.

*Ceramic specimens.* YBCO samples had the density $D/D_R = 0.33 - 0.92$ $(D_R = 6.38$ g/cm$^3$ is X-ray density) and $T_c = 85 - 92$ K.

TABLE

| N. | Composition, heat treatment | Structure, $\Delta = b - a$ (nm) | $T_c$ K | $H_v$ GPa | $K_{1c}$ MPa . m$^{1/2}$ | $P_{th}$ $10^{-2}$ N |
|---|---|---|---|---|---|---|
| 1 | | orthorhombic 0.070 | 85 | 7.3 | 0.38 | 1.5—2.0 |
| 2 | $YBa_2Cu_3O_{7-\delta}$ | orthorhombic | 60 | 9.7 | 0.57 | 2.5—5.0 |
| 3 | | orthorhombic | 70 | 5.5 | 0.48 | 1.0 |
| 4 | $YBa_2Cu_{3-x}Ti_xO_{7-\delta}$ x = 0.03 | orthorhombic 0.005 | 68 | 5.0 | 0.42 | 1.0—1.5 |
| 5 | quenched from 1173 K to air | tetragonal | | 6.9 | 0.34 | 1.5—2.0 |
| 6 | $GdBa_2Cu_3O_{7-\delta}$ | orthorhombic | 35 | 7.0 | 0.5 | 2.0 |
| 7 | annealed for 6hrs at 723 K in oxygen | orthorhombic | 55 | 7.0 | 0.5 | 2.0 |
| 8 | $HoBa_2Cu_3O_{7-\delta}$ | orthorhombic | 40 | 5.9 | 0.45 | 2.0 |
| 9 | $DyBa_2Cu_3O_{7-\delta}$ | orthorhombic | 50 | 5.7 | 0.4 | 1.0 |
| 10 | $ErBa_2Cu_3O_{7-\delta}$ | orthorhombic | *) | 5.8 | 0.5 | 1.0 |
| 11 | $YbBa_2Cu_3O_{3-\delta}$ | orthorhombic | 35 | 5.1 | 0.5 | 1.0 |

*) Superconductivity was not observed down to 4.2 K.

The Vickers microhardness, $H_v$, and the threshold stress intensity factor, $K_{1c}$, were estimated by the expressions:

$$H_v = 1.854 \, (P - P_{th})/(2a)^2 \quad \text{and} \quad K_{1c} = 0.1 \, (P - P_{th})/c^{3/2} \qquad (1)$$

where $P$ is the indentation load, $P_{th}$ is a threshold load [1]. $2a$ is the impression diagonal length, $c$ is the radial crack length near impression.

Microcreep of ceramics was studied employing a laser interferometer. Samples of cross section from $2 . 2$ to $4 . 4$ mm$^2$ and of height $6-10$ mm were compressed under stresses 10 to 12 MPa at temperature in the range 77 K $< T <$ 300 K. Destruction of the superconducting state was induced by passing a current. At 77 K the critical current density was $15-25$ A/cm$^2$.

(a) Microhardness and microbrittleness

*Single crystals*: When indenting the RBCO crystals, the impressions were observed on exceeding a threshold load $P_{th} = 0.025 - 0.05$ $N$ but for $P < P_{th}$ the strain was elastic. If the load was higher than 1 N, the samples were generally fractured [2].

The experimental data given in coordinates $(2a)^2 - P$ (see Fig. 1) are well described by a linear relation up to fracture load. This is true for $c^{3/2} - P$ dependence also. The straight lines cut off in the load axis the values less then $\simeq 0.04$ $N$ close to the above threshold loads.
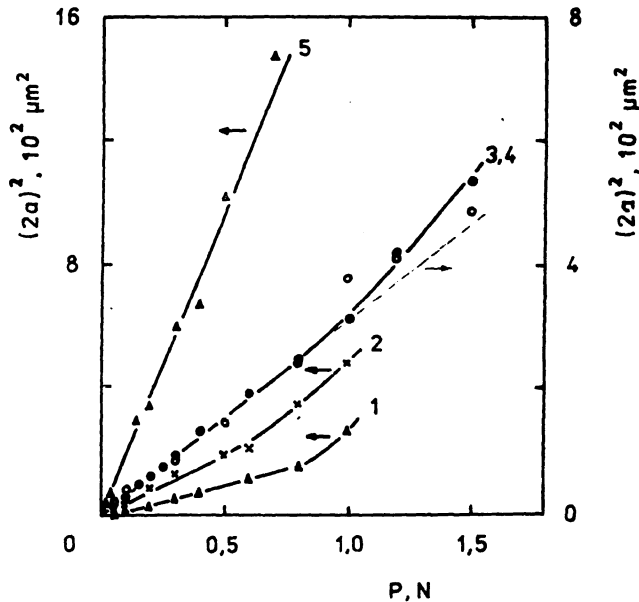


*Fig. 1.* Plots of impression diagonal length vs indentation load for YBaCuO (1- $T_c = 65$ K, 2 - $T_c = 90$ K), $La_{2-x}Sr_xCuO_4$ (3 - $T_c = 12$ K), $La_2CuO$ (4 - nonsupercond.) and BiSrCaCuO (5 - $T_c = 80$ K) single crystals.

Microhardness and fracture toughness of the single crystals studied are shown to vary within large ranges (see table). A certain correlation can be observed between the values of $H_v$ and $K_{1c}$: smaller values of $H_v$ are in conformity with smaller $K_{1c}$ values.

The study into mechanical anisotropy of HTSC single crystals reveals that the microhardness values are essentially identical for three basal planes and independent of indentation diagonal direction. By contract, the length and the direction of crack propagation are sensitive to identation crystallography. The planes of easy crack propagation are planes (100), (010), (001). For arbitrary diagonal orientations the cracks change smoothly their directions before the coincidence with [100] (Fig. 2).

When indenting the plane (001), the directions [010] and [100] of crack propagation are found to be equivalent. A high anisotropy of crack nucleation near impression was observed when indenting the planes (100) and (010). As shown in Fig. 2, the
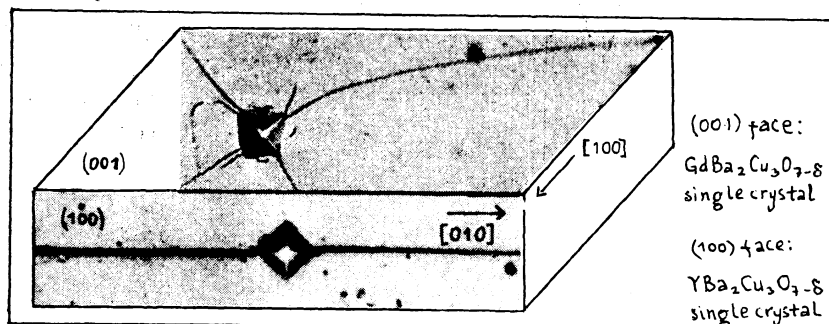


Fig. 2. Anisotropy of cracks propagation in RBCO. (001) face: GdBaCuO and (100) face: YBaCuO single crystals.

cracks propagate mainly in the plane (001) which seems to be characterized by a minimum surface energy. Noto that this is consistent with the observed growth of crystals in the form of thin plates parallel to the plane (001).

The micromechanical properties of Bi-containing HTSC crystals have been recently studied and reported by LUBENETS [4]. It should be noted that unlike crystals YBCO, the Bi-Sr-Ca-Cu-O crystals demonstrate highly nonuniform micro-mechanical properties because due to their multiphase nature. The microhardness was found to have tree typical values: 0.5, 1.1 and 3.1 GPa. These are considerably lower than the $H_v$ values obtained for crystals YBCO.

Other features of the Bi-Sr-Ca-Cu-O crystals are the lack of radial cracks and the formation of secondary crycks with a plane parallel to (001). These crystals appear to be more ductile than YBCO ones. The residual strain near indentation is no less than 1 %.

*Ceramics*: Density dependence of microhardness at room temperature is satisfactorily described by the empirical equation [5].

$$H_v = H_{v0} \exp\left[-n(1 - D/D_R)\right], \qquad (2)$$

where $H_{v0} = 4.5$ GPa, $n = 4.6$. The equ. 2 has been long since used to treat the effect of porosity on strength of different ceramic materials $(n = 4-7)$ [6].

The HTSC ceramics microhardness appears to be temperature dependent (Fig. 3). $H_v$ increases by $\simeq 50-80$ % with reducing temperature from 300 to 77 K. The relative increase of the microhardness is the stronger the higher indentation load. This may be due to an intergrain slip contribution to local strain. For low indentation loads, $H_v$ is closer to microhardness of a separate grain. Certain softening of the

134

ceramics (for $P = N$) can be observed near 200 K. The dependence $H_v(T)$ does not display the transition of ceramic to S-state within the limits of experimental accuracy.

(b) Microcreep

Figure 4 shows the creep curve of ceramics YBCO plotted as the strain rate $\dot{\varepsilon}(t)$. Creep of the ceramics was continuous for a long time although the rate varied. The
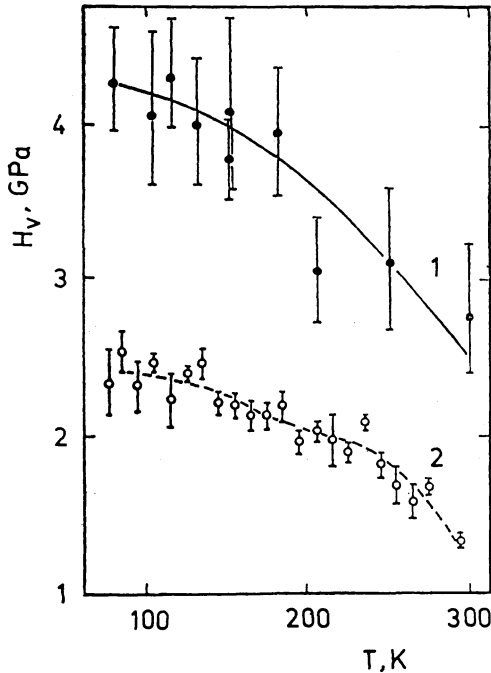


Fig. 3. Temperature dependence of micro-hardness for YBaCuO ceramics ($T_c = 92$ K, $D/D_R = 0.78$), (1): $P = 0.15$ $N$; (2): $P = 2.0$ $N$.
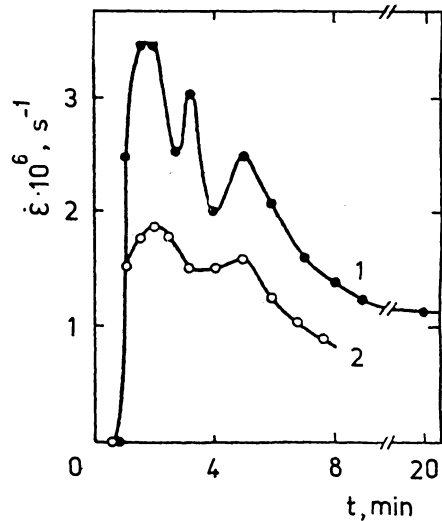
Fig. 4. Creep curves of ceramics YBaCuO at 77 K (1) and 250 K (2). Applied stress $\sigma = 10$ MPa.

following features of the deformation of ceramics were observed under a constant load: 1) an initial period when $\dot{\varepsilon}$ was close to zero; 2) a subsequent increase of $\dot{\varepsilon}$ which changed to weak fall of the rate; 3) absence of a steady-state creep stage; 4) short-term accelerations and slowing down of the deformation process corresponding to displacements by $\sim 1$ $\mu$m.

We investigated in more detail the process of deformation at 77 K, particularly the influence of the S-N and N-S transitions on the process. When the current was higher than the critical value, an interferogram always exhibited slowing down or arrest of the deformation process (Fig. 5).

Acceleration of the strain as a result of the N-S transition can be explained by

assuming that the motion of the twin boundaries in the $S$ state is facilitated by the absence of the electron drag [7].

The temperature dependence of the strain rate $\dot{\varepsilon}$, measured after a certain time from the application of a load or after passing through a given value of the strain, will be called the temperature spectrum of the strain rates.

Figure 6 shows typical inelastic deformation spectra of Y-ceramics [8]: one for a fine-grained ceramic with the grain size $1-3$ $\mu$m (curve 1); another which was a multi-phase coarse-grained ceramic with a grain size $10-30$ $\mu$m (curve 4); two spectra (curve 2 and 3) were recorded for single-phase coarse-grained samples from different batches demonstrating that, for the same values of $T_c$ and slightly different densities ($5.5$ g/cm$^3$ for sample 2 and $5.8$ g/cm$^3$ for sample 3), there were considerable differences between the strain rates at the maxima, whereas the temperatures of the maxima were practically the same.

It follows from Fig. 6 that out of the three peaks present in all the spectra the one located close to $T_c$ at $T_{max1} \cong 90$ K. The highest-temperature peak occurred at $T_{max2} = 250-270$ K.

It is known at present that the temperature dependences of various properties of high-temperature superconductors exibit anomalies near $T_c$ (the Young modulus, vibration decrement, and linear expansion coefficient). Clearly, these effects are of an identical origin to that described in the present paper.

Above the superconducting transition temperature there are also special features in some physical properties of HTSCs, which are attributed to structural changes (phase transitions or nucleation and motion of twins). The characteristic features
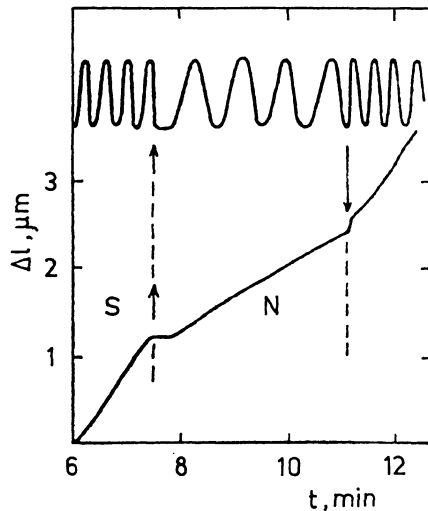


*Fig. 5.* Interferogram (top trace) and creep curve of ceramic YBaSrCuO at 77 K under a stress $\sigma = 12$ MPa calculated from the interferogram. The arrows identify the moments when a current of density $j = 25$ A/cm$^2$ was switched on and off.
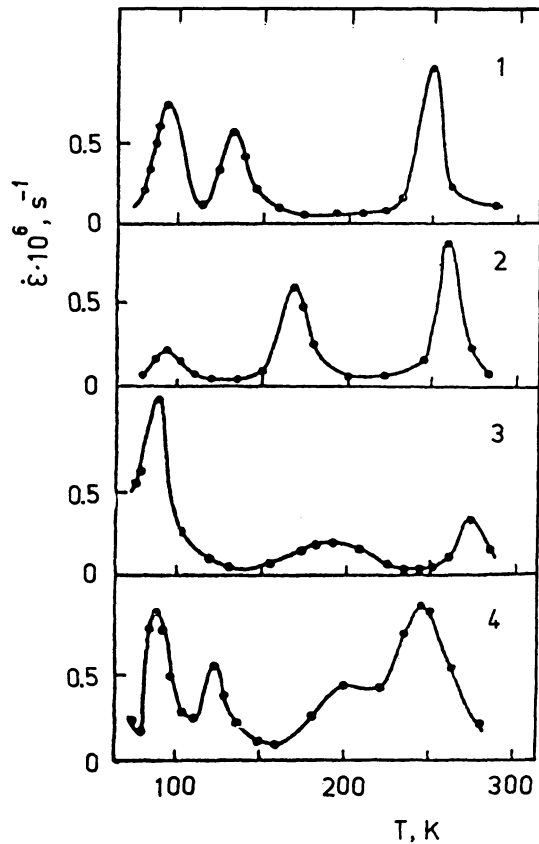
*Fig. 6.* Spectra of the rates of inelastic deformation by compression of YBaCuO ceramics;
$\sigma = 10 \, \text{MPa}$.

of the temperature spectrum of the strain rate are in qualitative agreement with the characteristics of the elasticity and specific heat.

The origin of the maxima, the mechanisms, and „carriers" of deformation in the ceramics must be investigated further.

### References

[1] Hays, E. G. and Kendall, E. G., Metallograph. 6, 1973, 275.

[2] Peschanskaya, N. N. et al., Mekh. Polim., N. 2, 1977, 357.

[3] Demirsky, V. V. et al., Fiz. Tverd. Tela, 6, 1989, 263.

[4] Lubenets, S. V., Sverchprovodimosť 3, 1990, N. 8 (part 2).

[5] Demirsky, V. V. et al., Sverchprovodimosť 3, 1990, 84.

[6] Kingery, W. D., „Introduction to ceramics", John Wiley and Sons, London, Isd. Liter. po Stroit., Moskva, 1967, 499 p.

[7] Peschanskaya, N. N. et al., Fiz. Tverd. Tela. 30, 1988, 2014.

[8] Peschanskaya, N. N. et al., Fiz. Tverd. Tela. 39, 1989, 271.